ULTRA SONO GRAPHY

ORIGINAL ARTICLE

https://doi.org/10.14366/usg.23106
eISSN: 2288-5943
Ultrasonography 2023;42:580-588

Utility of fusion imaging for the evaluation of ultrasound quality in hepatocellular carcinoma surveillance

Yeun-Yoon Kim[1]*, Seo-Bum Cho[1], Jae Seung Lee[2], Hye Won Lee[2], Jin-Young Choi[1], Seung Up Kim[2]

[1]Department of Radiology and Research Institute of Radiological Science, [2]Department of Internal Medicine and Institute of Gastroenterology, Severance Hospital, Yonsei University College of Medicine, Seoul, Korea

Purpose: This study evaluated the quality of surveillance ultrasound (US) for hepatocellular carcinoma (HCC) utilizing fusion imaging.

Methods: This research involved a secondary analysis of a prospectively recruited cohort. Under institutional review board approval, participants referred for surveillance US who had undergone liver computed tomography (CT) or magnetic resonance imaging (MRI) within the past year were screened between August 2022 and January 2023. After patient consent was obtained, the US visualization score in the Liver Imaging Reporting and Data System was assessed with fusion imaging at the time of examination. This score was compared to that of conventional US using the extended McNemar test. Multivariable logistic regression analysis was used to identify factors independently associated with a US visualization score of B or C. Factors limiting visualization of focal lesions were recorded during fusion imaging.

Results: Among the 105 participants (mean age, 59±11 years; 66 men), US visualization scores of B and C were assigned to 57 (54.3%) and 17 (16.2%) participants, respectively, by conventional US and 54 (51.4%) and 32 (30.5%) participants, respectively, by fusion imaging. The score distribution differed significantly between methods (P=0.010). Male sex was independently associated with US visualization scores of B or C (adjusted odds ratio, 3.73 [95% confidence interval, 1.30 to 10.76]; P=0.015). The most common reason (64.5%) for lesion non-detection was a limited sonic window.

Conclusion: Conventional US may underestimate the limitations of the sonic window relative to real-time fusion imaging with pre-acquired CT or MRI in the surveillance of HCC.

Keywords: Ultrasonography; Chronic disease surveillance; Hepatocellular carcinoma; X-ray computed tomography; Magnetic resonance imaging

Key points: Fusion imaging facilitates the evaluation of ultrasound (US) visualization score with reference to fused computed tomography or magnetic resonance imaging. Male sex was independently associated with a US visualization score of B or C. The most common reason for the non-detection of lesions during fusion imaging was a limited sonic window.

Received: May 31, 2023
Revised: August 11, 2023
Accepted: August 15, 2023

Correspondence to:
Jin-Young Choi, MD, PhD, Department of Radiology and Research Institute of Radiological Science, Severance Hospital, Yonsei University College of Medicine, 50-1 Yonsei-ro, Seodaemun-gu, Seoul 03722, Korea

Tel. +82-2-2228-7400
Fax. +82-2-393-3035
E-mail: gafield2@yuhs.ac

Seung Up Kim, MD, PhD, Department of Internal Medicine and Institute of Gastroenterology, Severance Hospital, Yonsei University College of Medicine, 50-1 Yonsei-ro, Seodaemun-gu, Seoul 03722, Korea

Tel. +82-2-2228-1944
Fax. +82-2-393-6884
E-mail: ksukorea@yuhs.ac

*Current address: Department of Radiology and Center for Imaging Sciences, Samsung Medical Center, Seoul, Korea

How to cite this article:
Kim YY, Cho SB, Lee JS, Lee HW, Choi JY, Kim SU. Utility of fusion imaging for the evaluation of ultrasound quality in hepatocellular carcinoma surveillance. Ultrasonography. 2023 Oct;42(4):580-588.

Introduction

Hepatocellular carcinoma (HCC) surveillance is implemented to improve the outcomes of high-risk individuals and to detect HCC in its early stages [1]. A primary imaging modality recommended for this surveillance is liver ultrasound (US) [2]. However, the sensitivity of liver US is widely known to be limited in the detection of early-stage HCC. A recent meta-analysis revealed that the sensitivity of early-stage HCC detection using US alone was 45%, which is quite low [3]. The low detection sensitivity of US is closely associated with inadequate US quality [4–6]. Several factors contribute to insufficient US quality, including a high body mass index and the presence of fatty liver [7]. Furthermore, due to the physical properties of the US beam, nearby structures such as the lungs, bowel, and rib cage can hamper the visualization of the liver [4].

In the US Liver Imaging Reporting and Data System (LI-RADS), the technical quality of US for HCC screening or surveillance is assessed using a US visualization score. This score is based on a 3-point scale: A represents no or minimal limitations, B indicates moderate limitations, and C signifies severe limitations [8]. A recent study, based on the analysis of over 10,000 US examinations conducted in the United States, revealed that 24% of the examinations had a visualization score of B, while 4% had a score of C [9]. This finding aligns with a meta-analysis showing that approximately one-quarter of US examinations exhibited limited examination quality [7]. However, in previous studies, the US visualization score has been evaluated by retrospectively reviewing captured images and reports [9–11], which can yield results that differ from those of on-site assessments [12]. Furthermore, even when the US visualization score is evaluated during the examination, inherent limitations exist to estimating the area of the liver that is not visible, due to the absence of a reference standard.

The technique of fusion imaging facilitates the alignment of anatomical coordinates between real-time US and previously acquired computed tomography (CT) or magnetic resonance imaging (MRI) thereby enabling side-by-side visualization of the same area on a monitor [13]. Fusion imaging serves as a valuable tool for guiding liver biopsy or ablation procedures, as it aids in the accurate localization of liver lesions observed on CT or MRI during US examination [14,15]. Since cross-sectional imaging with CT or MRI scans the entire liver, it is anticipated that the CT or MRI images in the fused state can serve as a reference standard for anatomical coverage of the liver during US examination. Consequently, this study was designed to evaluate the quality of US examinations for HCC screening or surveillance using fusion imaging.

Materials and Methods

Compliance with Ethical Standards

This study was approved by the Institutional Review Board of Severance Hospital (IRB No. 4-2022-0783). Written informed consent was obtained from all participants included in the study.

Participants

This study consisted of a secondary analysis of a prospectively recruited cohort. Under institutional review board approval, participants with chronic hepatitis B, chronic hepatitis C, or liver cirrhosis, who were referred for screening or surveillance US to the radiology department between August 2022 and January 2023, were screened. Those who had undergone CT or MRI of the entire liver within the past year were considered eligible. Participants were excluded if they declined to undergo additional US with fusion imaging, had a history of liver surgery, had undergone cardiac pacemaker implantation (these patients were excluded to mitigate potential adverse effects of electromagnetic tracking-based image fusion on the cardiac device) [16,17], or were unable to fast.

Fusion US Examination

The liver was examined using fusion imaging, in addition to conventional upper abdominal US, after a minimum fasting period of 6 hours. The fusion US was conducted by a board-certified radiologist (Y.-Y.K., with 4 years of practice experience) using one of the following systems: LOGIQ E9 volume navigation (GE Healthcare, Milwaukee, WI, USA), Aplio i800 Smart Fusion (Canon Medical Systems Corporation, Tokyo, Japan), or EPIQ 5 PercuNav Auto Registration (Philips Healthcare, Eindhoven, The Netherlands). A position sensor was mounted on the convex probe, and point registration was repeatedly performed using vascular or lesion landmarks to reduce misregistration in each hepatic segment.

Using fusion imaging, the operator evaluated several variables at the time of examination. Registration quality was documented based on the following criteria: a score of "excellent" denoted near-perfect registration for both the center and periphery of the liver; "acceptable" indicated successful registration for both the center and periphery, albeit with some misregistration; and "poor" referred to successful registration for the center, but with substantial misregistration for the periphery [18]. The presence and degree of fatty liver were evaluated as follows: "mild" referred to a slight increase in the echogenicity of the liver compared to the normal renal cortex; "moderate" denoted a moderate increase in the liver's echogenicity with mildly impaired visualization of intrahepatic vessels; and "severe" indicated a marked increase in the liver's echogenicity, with poor visualization of the right posterior

section parenchyma, intrahepatic vessels, and diaphragm [19]. The echotexture of the liver was classified as either heterogeneous, characterized by the presence of numerous nodules measuring 3 mm or more in the parenchyma, or homogeneous, characterized by a fine parenchymal echo with no such nodules [4]. The US visualization score in LI-RADS was recorded with reference to the fused CT or MRI images as follows: a score of A referred to US quality in which the majority of the liver was well visualized; B denoted US quality in which the liver echogenicity was moderately heterogeneous, or the US beam was moderately attenuated by fatty liver or other structures; and C indicated US quality in which the liver echogenicity was severely heterogeneous, or the US beam was significantly attenuated by fatty liver or other structures, resulting in over 50% of the liver not being visualized [8]. The visualization score of each segment was recorded in the same manner, and anatomical structures limiting visualization of the liver were noted according to the hepatic segment. The scan time for the liver was calculated by subtracting the time of generation of the first image from that of the last image.

In participants who had a focal lesion of 5 mm or larger, as identified on pre-acquired CT or MRI scans, the segment, size, and nature of the index lesion were recorded by a second-year radiology resident (S.-B.C.) prior to fusion imaging. During the fusion imaging process, the visibility of the lesions and any factors limiting visualization were noted. The US LI-RADS category was also recorded using the following scale: 1, no observation or only a definitively benign observation; 2, an observation of less than 10 mm that was not definitively benign; 3, an observation of 10 mm or larger that was not definitively benign, or the presence of a new tumor in the veins [8].

Conventional US Examination

Conventional US was performed by a radiology resident or radiologist of varying experience levels. For comparison with fusion imaging, the images from the same round of conventional US were retrospectively analyzed by a board-certified radiologist (J.-Y.C., with over 20 years of practice experience). This radiologist determined the US visualization score based on the LI-RADS, without knowledge of the fusion imaging results [8]. The same radiologist also retrospectively recorded the liver scan time in the same manner as with fusion US.

Statistical Analysis

Continuous variables were summarized using either the mean and standard deviation or the median and interquartile range (IQR). These were then compared using the Mann-Whitney U test, depending on the normality of the data. Categorical variables were summarized as counts and percentages and compared using either the chi-square test or the Fisher exact test. The distribution of the US visualization score between conventional and fusion US was compared using the extended McNemar test, with a type I error rate set at 0.05. For a power of 80% and a sample size of 105 pairs, the minimum detectable ratio sum for discordant proportions was 0.10. This corresponds to a low effect size, as determined using the PASS 2022 power analysis and sample size software (version 22.0.1, NCSS LLC, Kaysville, UT, USA) [20]. Multivariable logistic regression analysis was performed to identify factors that were independently associated with a US visualization score of B or C. This was based on variables examined in a previous meta-analysis [7]. A two-sided P-value of less than 0.05 was considered to indicate statistical significance. Analyses were performed using the R package (version 3.6.3, The R Foundation for Statistical Computing, Vienna, Austria).

Results

Participants and US Characteristics

A total of 105 participants (mean age, 59±11 years; 66 men) were enrolled in the study (Table 1, Fig. 1). Most participants were infected with the hepatitis B virus (84.8%). Among the 40 participants with liver cirrhosis, 34 (85.0%) were classified as Child-Pugh A. Fusion imaging was primarily performed using either unenhanced MRI (48.6%) or enhanced CT (45.7%). The previous CT or MRI used for fusion imaging was typically obtained for alternative surveillance (72.4%) or for follow-up on extrahepatic malignancy (19.1%). In addition to the approximately 2 minutes required for image fusion between real-time US and pre-acquired CT/MRI, the median scan time for fusion US was 4 minutes (IQR, 3 to 5 minutes),

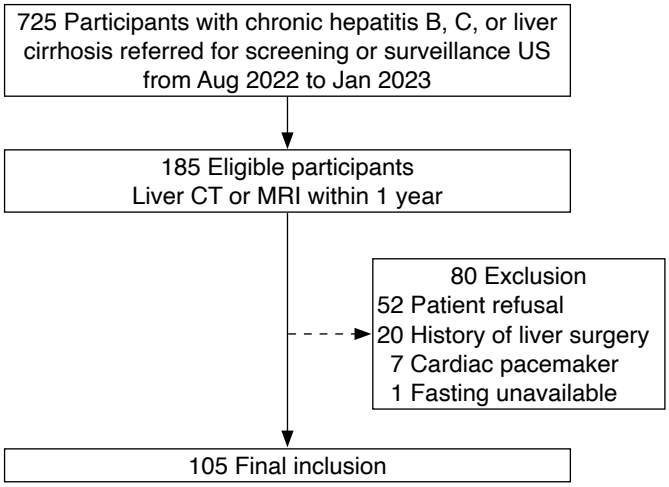

Fig. 1. Flow diagram of participant enrollment. CT, computed tomography; MRI, magnetic resonance imaging; US, ultrasound.

Table 1. Participant and examination characteristics

Characteristic	Value (n=105)
Age (year)	59±11
Male sex	66 (62.9)
BMI (kg/m^2)	24.2 (22.6–26.4)
DM	23 (21.9)
Etiology of liver disease	
HBV	88 (83.8)
HCV	1 (1.0)
HBV and HCV	1 (1.0)
Alcohol	10 (9.5)
Non-B, non-C, non-alcohol	5 (4.8)
History of HCC	6 (5.7)
Aspartate aminotransferase (IU/L)	27 (23–34)
Alanine aminotransferase (IU/L)	21 (16–29)
Albumin (g/dL)	4.5 (4.3–4.7)
INR (n=86)	0.98 (0.95–1.03)
Total bilirubin (mg/dL)	0.9 (0.6–1.1)
Creatinine (mg/dL)	0.85 (0.73–0.97)
Platelet (×10^9/L) (n=94)	183.05±64.08
Serum AFP (ng/mL) (n=98)	2.55 (1.35–4.10)
Fusion modality	
Unenhanced/enhanced MRI	51 (48.6)/3 (2.9)
Unenhanced/enhanced CT	3 (2.9)/48 (45.7)
Reason for previous CT or MRI	
Alternative surveillance	76 (72.4)
Follow-up for extrahepatic malignancy	20 (19.1)
Evaluation of other medical condition	7 (6.7)
Evaluation of hepatic nodule	2 (1.9)
Registration quality	
Excellent	43 (41.0)
Acceptable	59 (56.2)
Poor	3 (2.9)
Fatty liver on US	
None	56 (53.3)
Mild	31 (29.5)
Moderate	16 (15.2)
Severe	2 (1.9)
Liver echotexture	
Heterogeneous	31 (29.5)
Homogeneous	74 (70.5)
US visualization score by fusion US	
A (no or minimal limitations)	19 (18.1)
B (moderate limitations)	54 (51.4)
C (severe limitations)	32 (30.5)
US LI-RADS category	
1	97 (92.4)
2	5 (4.8)
3	3 (2.9)

Values are presented as mean±SD, number of participants (%), or median (IQR).
BMI, body mass index; DM, diabetes mellitus; HBV, hepatitis B virus; HCV, hepatitis C virus; HCC, hepatocellular carcinoma; INR, international normalized ratio; AFP, α-fetoprotein; MRI, magnetic resonance imaging; CT, computed tomography; US, ultrasound; LI-RADS, Liver Imaging Reporting and Data System; SD, standard deviation; IQR, interquartile range.

which was longer than that for conventional US (2 minutes [IQR, 2 to 3 minutes]) (P<0.001). Severe fatty liver was a rare occurrence, found in only 1.9% of participants, while 70.5% of participants exhibited a homogeneous echotexture of the liver. The majority of participants, 92.4%, were assigned to US LI-RADS category 1.

US Visualization Score

With the conventional US method, US visualization scores of A, B, and C were assigned to 31 (29.5%), 57 (54.3%), and 17 (16.2%) participants, respectively. However, when the fusion imaging techniques of US/MRI (n=54) or US/CT (n=51) were used, scores of A, B, and C were found in 19 (18.1%), 54 (51.4%), and 32 (30.5%) participants, respectively. This difference in score distribution between the two methods was statistically significant (P=0.010) (Fig. 2A). Furthermore, of the participants who received scores of A and B on conventional US, 5 (16.1%) and 19 (33.3%), respectively, were reassigned a score of C when evaluated using fusion imaging (Figs. 2B, 3).

The degree of limitation varied significantly based on the hepatic segment (P<0.001) (Table 2). The segmental visualization scores of B or C were most commonly observed in hepatic segments 7 and 8, followed by segments 5 and 6, and then segments 2 and 3. The score of C was most frequently seen in hepatic segments 7 and 8 (54.3%), primarily due to the lung and ribs. The lung obscured areas of segments 7 and 8 in 86.7% of cases, while the ribs impeded the visualization of various hepatic segments (Fig. 4).

Multivariable logistic regression analysis demonstrated an independent association between male sex and a US visualization score of B or C (adjusted odds ratio, 3.73 [95% confidence interval, 1.30 to 10.76]; P=0.015) (Table 3).

Detection of Focal Liver Lesions Noted on Previously Acquired CT or MRI

Among 60 participants with 109 focal liver lesions (median size, 7

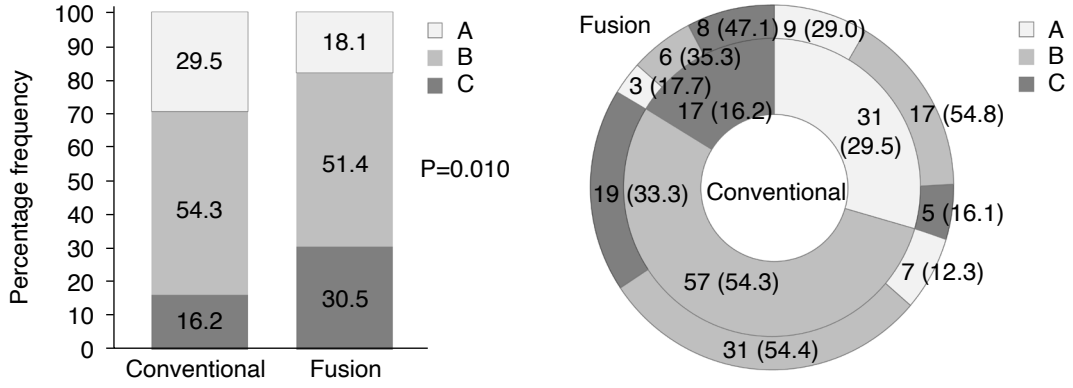

Fig. 2. Ultrasound (US) visualization score as evaluated by conventional and fusion US methods.
A. The bar graph illustrates the percentage frequency distribution of US visualization scores obtained using both US techniques. P-value was derived from a comparison of the proportions using the extended McNemar test. B. The nested pie chart displays the frequency and relative percentage of US visualization scores as determined by fusion US, within each sector of US visualization scores as determined by conventional US. The data are presented as numbers, with percentages shown in parentheses.

Table 2. Sonic window evaluation by fusion US according to hepatic segment

	Segment 1	Segment 4	Segments 2 and 3	Segments 5 and 6	Segments 7 and 8	P-value
Segmental visualization score						
A (no or minimal limitations)	86 (81.9)	74 (70.5)	58 (55.2)	45 (42.9)	7 (6.7)	<0.001
B (moderate limitations)	14 (13.3)	22 (21.0)	28 (26.7)	54 (51.4)	41 (39.1)	
C (severe limitations)	5 (4.8)	9 (8.6)	19 (18.1)	6 (5.7)	57 (54.3)	
Factors limiting visualization of the liver						
Rib	6 (5.7)	23 (21.9)	41 (39.1)	37 (35.2)	24 (22.9)	<0.001
Lung	0	2 (1.9)	0	14 (13.3)	91 (86.7)	<0.001
Colon	0	9 (8.6)	0	19 (18.1)	3 (2.9)	<0.001
Stomach	5 (4.8)	0	9 (8.6)	0	0	<0.001
Omentum	0	1 (1.0)	1 (1.0)	0	1 (1.0)	>0.999
Ligamentum venosum	8 (7.6)	0	0	0	0	<0.001
Fatty liver	0	0	0	0	2 (1.9)	0.199

Values are presented as number (%).
P-values were obtained using the chi-square test or the Fisher exact test.
US, ultrasound.

mm [IQR, 5 to 13 mm]), the lesions not detected on fusion US were significantly smaller than those that were detected (median size, 6 mm vs. 8 mm; P=0.005). Of the 31 lesions that were not detected on fusion US, the reason for non-detection was identified as a limited sonic window in 64.5% of cases. This was followed by small lesion size, accounting for 16.1% of non-detections, and fatty liver, which accounted for 12.9% (Table 4).

Discussion

In this secondary analysis of a prospectively recruited cohort, the technical quality of US for HCC screening or surveillance was evaluated based on the US LI-RADS at the time of examination. The anatomical coverage of the liver provided by real-time fusion imaging with pre-acquired CT or MRI, as well as the liver parenchymal echotexture and presence of fatty liver, were considered. Among 105 participants with chronic hepatitis B, chronic hepatitis C, or liver cirrhosis, 51.4% and 30.5% were assigned US visualization scores B and C, respectively, based on fusion imaging. Fusion imaging revealed that 16.1% and 33.3% of participants who initially received US visualization scores of A and B, respectively, on conventional US were reassigned a visualization score of C. This

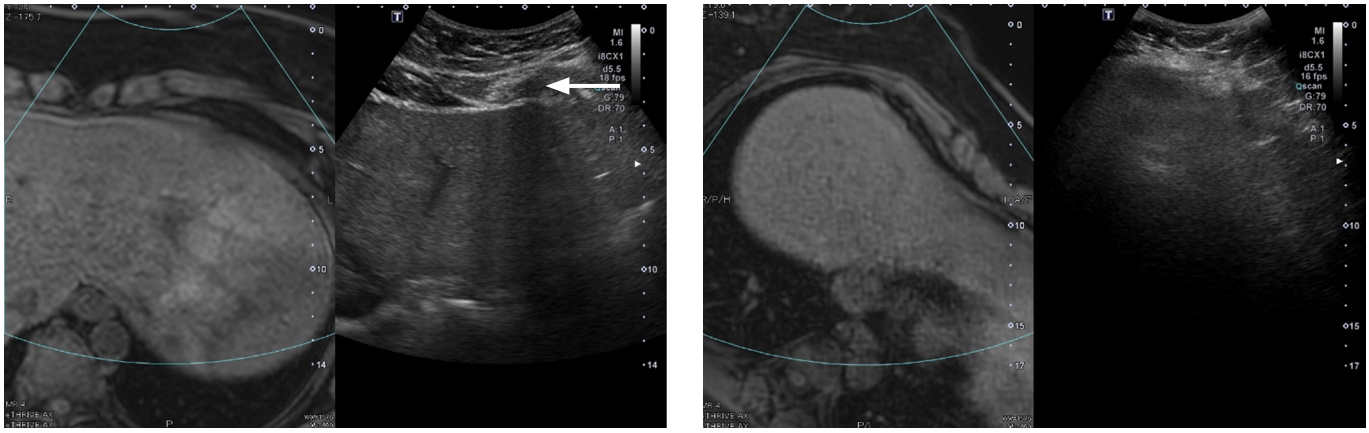

A B

Fig. 3. Discrepant ultrasound (US) visualization scoring between fusion imaging and conventional US in a 40-year-old woman with chronic hepatitis B virus infection and a body mass index of 28.1 kg/m^2.
Fusion US reveals severe limitations in the visualization of segments 2 and 3 due to the rib (arrow) on the subcostal view (A) and of segments 7 and 8 due to the lung on the intercostal view (B). The US visualization score was rated as C by fusion US and B by conventional US.

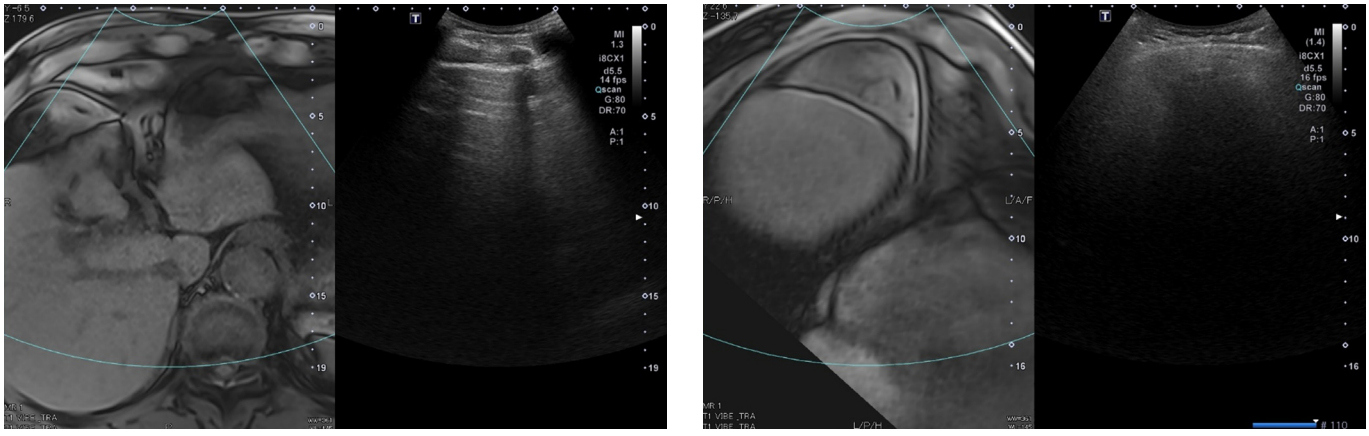

A B

Fig. 4. Concordant ultrasound (US) visualization scoring between fusion imaging and conventional US in a 79-year-old man with alcoholic liver cirrhosis and a body mass index of 25.4 kg/m^2.
Fusion US reveals severe limitations in the visualization of the entire liver on the subcostal view (A) and of segments 7 and 8 due to the rib (B). A US visualization score C was assigned by both fusion US and conventional US. Fusion US was instrumental in documenting the areas of the liver that were not visible.

Table 3. Factors associated with a US visualization score of B or C as determined by fusion US

	Univariable		Multivariable	
	OR (95% CI)	P-value	OR (95% CI)	P-value
Male sex	3.75 (1.33–10.57)	0.013	3.73 (1.30–10.76)	0.015
Age ≥60 years	0.82 (0.30–2.22)	0.696	0.90 (0.32–2.57)	0.845
Liver disease etiology other than HBV	1.65 (0.34–7.97)	0.531	1.29 (0.24–6.95)	0.766
BMI ≥25 kg/m^2	0.90 (0.33–2.46)	0.836	0.92 (0.31–2.73)	0.886
Moderate to severe fatty liver	4.43 (0.55–35.58)	0.161	4.25 (0.49–37.31)	0.191

US, ultrasound; OR, odds ratio; CI, confidence interval; HBV, hepatitis B virus; BMI, body mass index.

Table 4. Lesion characteristics

	Value (n=109)
Size (mm), median (IQR)	7 (5–13)
Location	
Segments 2 or 3	27 (24.8)
Segment 4	12 (11.0)
Segments 5 or 6	36 (33.0)
Segments 7 or 8	34 (31.2)
Entity	
Cyst	75 (68.8)
Hemangioma	17 (15.6)
Dysplastic or FNH-like nodule	5 (4.6)
Calcification	4 (3.7)
Treated lesion	3 (2.8)
Indeterminate lesion	3 (2.8)
Arterioportal shunt	2 (1.8)
Reason for non-detection	n=31
Limited sonic window	20 (64.5)
Small lesion size	5 (16.1)
Fatty liver	4 (12.9)
Pseudolesion	2 (6.5)

Values are presented as number of lesions (%) unless otherwise indicated.
IQR, interquartile range; FNH, focal nodular hyperplasia.

suggests that conventional US may underestimate the limitations of the sonic window.

Several points should be considered in the interpretation of these study results. First, our analysis reveals a significantly different distribution of US visualization scores compared to previous reports, which indicated proportions of scores B and C of 14.4%–24.2% and 2.5%–4.2%, respectively [9,21,22]. In the present study, the proportions of scores of B and C on conventional US were even higher (54.3% and 16.2%, respectively) than those in previous studies focused on patients with liver cirrhosis (27.5% and 28.0%, respectively) or chronic hepatitis B (50% and 1%, respectively) [5,10]. Notably, among the present participants, 72.4% had undergone CT or MRI for alternative surveillance. The quality of surveillance US in prior rounds in these participants may have been deemed inadequate, prompting the use of alternative surveillance methods. This could potentially introduce selection bias [5]. Furthermore, on-site comparison with CT or MRI revealed that a retrospective review of captured images from conventional US may underestimate the areas of the liver that are not visible. It is important to highlight that retrospective evaluation of US quality based on captured images can pose challenges [12]. The use of real-time fusion imaging with CT or MRI as a reference standard for anatomical coverage could potentially offer a more accurate evaluation of US quality following alternative surveillance with CT or MRI.

Male sex was found to be independently associated with US visualization scores of B or C, indicative of inadequate US quality. This finding aligns with previous research [23]. One possible explanation for this association is the higher frequency of rib shadowing in male patients [23], a factor that, in the present study, led to sonic window limitations across nearly all hepatic segments. Previous research has also suggested an association between fatty liver and suboptimal US quality [7]. However, the present study did not corroborate this, potentially due to the limited number of participants with severe fatty liver. Nevertheless, US beam attenuation did hinder the visualization of liver parenchyma or index lesions, which could contribute to suboptimal US quality.

The detectability of focal lesions, as identified on pre-existing CT or MRI scans, was evaluated using fusion imaging to ascertain the potential reasons for their non-detection on US. Notably, most of these lesions were either cysts or hemangiomas—which exhibit different echogenicity from HCC on US—and were less than a centimeter in size. The most common reason for non-detection on fusion US was the limited sonic window. These findings align with a previous study that demonstrated a lower detectability of lesions when the US visualization score was B or C, as opposed to A [24]. Moreover, the failure to detect HCC during US surveillance was associated with areas of the liver that were not visible [25]. The unseen areas identified in that study, such as the hepatic dome and the subcapsular area beneath the ribs, coincide with the locations assigned with segmental visualization scores of B and C in the present study. Consequently, areas obscured by the lung or ribs should be examined carefully during US surveillance.

Several studies have indicated that alternative imaging modalities, such as CT or MRI, may effectively increase detection sensitivity during HCC surveillance [26–28]. While a longitudinal follow-up study of these participants has not yet been conducted, the use of fusion imaging could assist in identifying patients who might benefit from alternative surveillance due to insufficient US quality. For patients who are undergoing alternative surveillance with gadoxetic acid-enhanced MRI, the application of US/MRI fusion could be beneficial in monitoring MRI-identified hepatobiliary phase hypointense nodules, which carry a high risk of progressing to advanced HCC [29]. Future studies are warranted to validate these concepts.

This study does present several limitations. First, the requirement for prior CT or MRI scans as an eligibility criterion may have led to selection bias. As previously noted, participants with substandard US quality may have been overrepresented. Second, interobserver

variability could not be assessed for US visualization scoring, as only one operator performed the fusion imaging. It is also possible that the US visualization score may change dynamically; further research is necessary to validate the findings. Third, operator experience with conventional US could vary, leading to inconsistencies in the acquisition of US images. This could potentially affect the comparison with fusion imaging. Fourth, this study did not account for changes in patient position, such as a semi-erect position, which is used to improve visualization of the entire liver [30]. Given the technical difficulties of applying fusion imaging in various patient positions, this issue may be outside the scope of the present study. Further research is needed to investigate the US visualization score in relation to fusion imaging, taking into account patient position. Finally, the general applicability of the findings may be somewhat restricted due to the predominance of hepatitis B virus infection among the study participants.

In conclusion, the use of real-time fusion imaging, with CT or MRI as the reference standard for anatomical coverage, may provide a more accurate assessment of US quality in HCC surveillance, especially after alternative surveillance methods have been employed.

ORCID: Yeun-Yoon Kim: https://orcid.org/0000-0003-2018-5332; Seo-Bum Cho: https://orcid.org/0009-0002-4158-2038; Jae Seung Lee: https://orcid.org/0000-0002-2371-0967; Hye Won Lee: https://orcid.org/0000-0002-3552-3560; Jin-Young Choi: https://orcid.org/0000-0002-9025-6274; Seung Up Kim: https://orcid.org/0000-0002-9658-8050

Author Contributions

Conceptualization: Kim YY, Choi JY, Kim SU. Data acquisition: Kim YY, Cho SB, Lee JS, Lee HW, Choi JY, Kim SU. Data analysis or interpretation: Kim YY, Choi JY, Kim SU. Drafting of the manuscript: Kim YY. Critical revision of the manuscript: Cho SB, Lee JS, Lee HW, Choi JY, Kim SU. Approval of the final version of the manuscript: all authors.

Conflict of Interest

No potential conflict of interest relevant to this article was reported.

Acknowledgments

This study was supported by the Research Fund of the Korean Society of Ultrasound in Medicine for 2022.

References

1. Singal AG, Pillai A, Tiro J. Early detection, curative treatment, and survival rates for hepatocellular carcinoma surveillance in patients with cirrhosis: a meta-analysis. PLoS Med 2014;11:e1001624.
2. Korean Liver Cancer Association (KLCA); National Cancer Center (NCC) Korea. 2022 KLCA-NCC Korea practice guidelines for the management of hepatocellular carcinoma. Korean J Radiol 2022;23:1126-1240.
3. Tzartzeva K, Obi J, Rich NE, Parikh ND, Marrero JA, Yopp A, et al. Surveillance imaging and alpha fetoprotein for early detection of hepatocellular carcinoma in patients with cirrhosis: a meta-analysis. Gastroenterology 2018;154:1706-1718.
4. Kim YY, An C, Kim DY, Aljoqiman KS, Choi JY, Kim MJ. Failure of hepatocellular carcinoma surveillance: inadequate echogenic window and macronodular parenchyma as potential culprits. Ultrasonography 2019;38:311-320.
5. Park MK, Lee DH, Hur BY, Lee HC, Lee YB, Yu SJ, et al. Effectiveness of US surveillance of hepatocellular carcinoma in chronic hepatitis B: US LI-RADS visualization score. Radiology 2023;307:e222106.
6. Kim DH, Choi JI. Current status of image-based surveillance in hepatocellular carcinoma. Ultrasonography 2021;40:45-56.
7. Hong SB, Kim DH, Choi SH, Kim SY, Lee JS, Lee NK, et al. Inadequate ultrasound examination in hepatocellular carcinoma surveillance: a systematic review and meta-analysis. J Clin Med 2021;10:3535.
8. Morgan TA, Maturen KE, Dahiya N, Sun MR, Kamaya A; American College of Radiology Ultrasound Liver Imaging Reporting Data System Working Group. US LI-RADS: ultrasound Liver Imaging Reporting and Data System for screening and surveillance of hepatocellular carcinoma. Abdom Radiol (NY) 2018;43:41-55.
9. Fetzer DT, Browning T, Xi Y, Yokoo T, Singal AG. Associations of ultrasound LI-RADS visualization score with examination, sonographer, and radiologist factors: retrospective assessment in over 10,000 examinations. AJR Am J Roentgenol 2022;218:1010-1020.
10. Son JH, Choi SH, Kim SY, Jang HY, Byun JH, Won HJ, et al. Validation of US Liver Imaging Reporting and Data System version 2017 in patients at high risk for hepatocellular carcinoma. Radiology 2019;292:390-397.
11. Tiyarattanachai T, Bird KN, Lo EC, Mariano AT, Ho AA, Ferguson CW, et al. Ultrasound Liver Imaging Reporting and Data System (US LI-RADS) visualization score: a reliability analysis on inter-reader agreement. Abdom Radiol (NY) 2021;46:5134-5141.
12. Kutaiba N, Ardalan ZS. Limitations associated with assessing liver ultrasound quality using US LI-RADS visualization score when utilizing acquired images. Clin Gastroenterol Hepatol 2022;20:1617-1618.
13. European Society of Radiology (ESR). Abdominal applications of ultrasound fusion imaging technique: liver, kidney, and pancreas. Insights Imaging 2019;10:6.
14. Lee MW. Fusion imaging of real-time ultrasonography with CT or MRI for hepatic intervention. Ultrasonography 2014;33:227-239.

15. Ahn SJ, Lee JM, Lee DH, Lee SM, Yoon JH, Kim YJ, et al. Real-time US-CT/MR fusion imaging for percutaneous radiofrequency ablation of hepatocellular carcinoma. J Hepatol 2017;66:347-354.
16. Beinart R, Nazarian S. Effects of external electrical and magnetic fields on pacemakers and defibrillators: from engineering principles to clinical practice. Circulation 2013;128:2799-2809.
17. Minami Y, Kudo M. Ultrasound fusion imaging technologies for guidance in ablation therapy for liver cancer. J Med Ultrason (2001) 2020;47:257-263.
18. Han S, Lee JM, Lee DH, Yoon JH, Chang W. Utility of real-time CT/MRI-US automatic fusion system based on vascular matching in percutaneous radiofrequency ablation for hepatocellular carcinomas: a prospective study. Cardiovasc Intervent Radiol 2021;44:1579-1596.
19. Strauss S, Gavish E, Gottlieb P, Katsnelson L. Interobserver and intraobserver variability in the sonographic assessment of fatty liver. AJR Am J Roentgenol 2007;189:W320-W323.
20. Chow SC, Shao J, Wang H, Lokhnygina Y. Sample size calculations in clinical research. 3rd ed. Boca Raton, FL: Taylor & Francis Group, 2018.
21. Millet JD, Kamaya A, Choi HH, Dahiya N, Murphy PM, Naveed MZ, et al. ACR ultrasound Liver Reporting and Data System: multicenter assessment of clinical performance at one year. J Am Coll Radiol 2019;16:1656-1662.
22. Tiyarattanachai T, Fetzer DT, Kamaya A. Multicenter study of ACR ultrasound LI-RADS visualization scores on serial examinations: implications for surveillance strategies. AJR Am J Roentgenol 2022;219:445-452.
23. Simmons O, Fetzer DT, Yokoo T, Marrero JA, Yopp A, Kono Y, et al. Predictors of adequate ultrasound quality for hepatocellular carcinoma surveillance in patients with cirrhosis. Aliment Pharmacol Ther 2017;45:169-177.
24. Kang JH, Choi SH, Kim SY, Lee SJ, Shin YM, Won HJ, et al. US LI-RADS visualization score: diagnostic outcome of ultrasound-guided focal hepatic lesion biopsy in patients at risk for hepatocellular carcinoma. Ultrasonography 2021;40:167-175.
25. Lee J, Park SB, Byun S, Kim HI. Impact of ultrasonographic blind spots for early-stage hepatocellular carcinoma during surveillance. PLoS One 2022;17:e0274747.
26. Kim SY, An J, Lim YS, Han S, Lee JY, Byun JH, et al. MRI with liver-specific contrast for surveillance of patients with cirrhosis at high risk of hepatocellular carcinoma. JAMA Oncol 2017;3:456-463.
27. Gupta P, Soundararajan R, Patel A, Kumar MP, Sharma V, Kalra N. Abbreviated MRI for hepatocellular carcinoma screening: a systematic review and meta-analysis. J Hepatol 2021;75:108-119.
28. Pocha C, Dieperink E, McMaken KA, Knott A, Thuras P, Ho SB. Surveillance for hepatocellular cancer with ultrasonography vs. computed tomography: a randomised study. Aliment Pharmacol Ther 2013;38:303-312.
29. Park HJ, Lee TY, Kim SY, Kim MJ, Singal AG, Lee SJ, et al. Hypervascular transformation of hepatobiliary phase hypointense nodules without arterial phase hyperenhancement on gadoxetic acid-enhanced MRI: long-term follow-up in a surveillance cohort. Eur Radiol 2022;32:5064-5074.
30. Ko SE, Lee MW, Lim HK, Min JH, Cha DI, Kang TW, et al. The semi-erect position for better visualization of subphrenic hepatocellular carcinoma during ultrasonography examinations. Ultrasonography 2021;40:274-280.